RUSSIAN JOURNAL OF EARTH SCIENCES, VOL. 3, NO. 2, PAGES 125–144, MAY 2001

A gravity model of the North Eurasia crust and upper mantle: 1. Mantle and isostatic residual gravity anomalies

M. K. Kaban

Schmidt United Institute of Physics of the Earth, Russian Academy of Sciences, (UIPE RAS), Moscow

Abstract. A numerical density model of the North Eurasia crust is constructed and its gravity effect is calculated. This model includes variations in the thickness and density of the sedimentary cover and solid crust, derived from generalization of seismic and geological data and specified on a $1° \times 1°$ grid within (30°–75°N, 14°W–195°E). Residual mantle anomalies are calculated by removing the anomalous model field from the observed gravity field. The mantle anomalies are reliably separated into two components accounting for the effects of different factors: (1) The regional component does not correlate, in a first approximation, with crustal structures and reflects large-scale structural heterogeneities of the Eurasia lithosphere, supposedly related to its thermal regime. Intense positive anomalies characterize northern and central Eurasia, and negative anomalies are observed in Western Europe and Southeast Asia. The regional component is consistent with the shear wave velocity distribution obtained from seismic tomography data. (2) The local component of the mantle gravity field has wavelengths shorter than 2000–2500 km and evidently correlates with specific tectonic structures. Maximum positive anomalies with amplitudes exceeding 100 mGal characterize some structures of the East European platform (Baltic Shield and Voronezh Massif) and East Siberia (Tunguska syneclise). A chain of negative mantle anomalies is clearly traced west of the Tesseyre-Tornquist line (Pannonian basin-Rhine graben-Massif Central). In Central Asia the most prominent zone of negative mantle anomalies is located southwest of Lake Baikal, approximately in the Khamar-Daban Range area. These anomalies are likely to be related to intrusion of an anomalously hot and light mantle. The intense negative mantle anomalies observed along the eastern boundary of Eurasia are associated with backarc seas. A new map of the isostatic gravity anomalies is calculated throughout the territory studied. As distinct from previous studies, real data on the crustal structure, including variations in the thickness and density of the sedimentary cover and solid crust, were used for its calculation. The use of these data instead of the traditional Airy scheme has led in many cases to a revision of notions concerning the isostatic state of the crustal structures. In particular, as compared with previous maps, significantly reduced amplitudes of the isostatic anomalies are obtained for the South Caspian, Tien Shan and Urals regions.

Paper number TJE01062.
CCC: 0000–0000/2001/0302–00062$18.00

The online version of this paper was published August 21, 2001.
URL: http://rjes.agu.org/v03/TJE01062/TJE01062.htm
Print companion will be issued.

1. Introduction

Density inhomogeneities in the upper mantle related to variations in temperature and mineral composition provide one of the main driving forces of both vertical and horizontal motions of lithospheric blocks. Information on these inhomogeneities can be gained from the gravity field. Unfortunately, the observed gravity field contains signatures of nearly all heterogeneities of the Earth. Therefore, in order to extract the mantle component, all mantle-unrelated effects should be eliminated from the observed field as effectively as possible; first of all, this is the crust effect because it is, on the one hand, the largest and, on the other hand, can be fairly reliably determined from a priori (mainly seismic) data independent of the gravity field. The residual gravity anomalies which can be called, within the accuracy (reliability) of the initial model of the crust, the *mantle* anomalies are most suitable for geodynamic reconstructions and for determining the patterns and intensities of processes responsible for the evolution of the mantle and lithosphere.

Attempts to calculate mantle gravity anomalies were made since the first deep seismic sounding (DSS) profiles were measured, but a reliable 3-D model could only be constructed after sufficient initial data on the crustal structure had been accumulated. The first gravity model of the lithosphere including a considerable part of North Eurasia was constructed by *Artemjev et al.* [1993, 1994a, 1994b], but the data used by these authors have been largely outdated by now. In particular, data from long DSS profiles (in total, a few ten thousand kilometers) are available now; they have provided unique constraints on the structure of the crust and upper mantle in vast areas of Siberia and East European platform [*Egorkin,* 1998; *Kostyuchenko et al.,* 1999]. Moreover, *Artemjev et al.* [1993, 1994a, 1994b] did not conduct a comprehensive analysis of density inhomogeneities in the solid crust. Mantle anomalies in several regions of North Eurasia were calculated in a number of works. *Yegorova and Starostenko* [1999] analyzed a density model of the lithosphere under a part of the East European platform and Western Europe, but in some places (e.g. Baltic Shield) it is also based on outdated evidence on the crustal structure. A density model of the crust and upper mantle in southern regions of the former USSR was constructed in [*Kaban et al.,* 1998]. It is important to note that results of regional studies cannot be directly compared because they usually employ different technologies including different reference models, relations between density and velocity, and so on. Therefore, the construction of a new map of mantle gravity anomalies throughout the territory of North Eurasia, using the newest data on the crustal structure and based on a consistent approach, is a relevant problem.

Tectonic processes significantly affect near-surface structures and the result is a concentration of density inhomogeneities appearing on the surface as topographic forms. Gravity anomalies (primarily local ones) contain information on hidden inhomogeneities of the sedimentary cover and basement and on a configuration of fault zones. Crustal faults have long been known to be mostly associated with zones of higher horizontal gradients of gravity anomalies. Many researchers emphasized that the isostatic reduction of gravity anomalies is most sensitive to fracture zones in which earthquakes can occur [e.g. *Artemjev,* 1975]. At that time, any isostatic gravity anomaly was considered as evidence for an isostatic disturbance of the crust. Subsequent studies showed that the isostatic gravity anomalies do not necessarily reflect deviations from isostasy; *Grachev* [1972] appear to have been first to note this fact. Isostatic models of that time were very simple, being usually represented by Airy schemes with a priori chosen parameters such as the normal crustal thickness at the sea level and the density jump at the crust-mantle interface. These models did not include density inhomogeneities within the crust and did not account for the variety of isostatic adjustment modes in various regions of the Earth. As a result, the inferred isostatic anomalies largely (as is clear now, predominantly) reflect, rather than deviations from isostasy, density variations in the upper part of the geological section, e.g. due to variations in thickness and density of sediments.

The development of isostatic studies during the last two decades has resulted in the revision and updating of many conventional conceptions. First of all, models used for calculating isostatic gravity anomalies have been much complicated. In their case study of the Tien Shan region, *Artemyev and Golland* [1983] were first to show that the use of an isostatic compensation model consistent with the actual crustal structure allows one to significantly reduce the isostatic anomalies as compared with the anomalies calculated in terms of the standard Airy scheme. Presently, detailed data on the structure of the sedimentary cover and its physical characteristics are available in many regions (e.g. see [*Avchan and Ozerskaya,* 1985; *Bronguleev,* 1986; *Ermakov et al.,* 1989; *Nevolin and Kovylin,* 1993]); based on these data, many of the upper crust density inhomogeneities can be incorporated into the model. Additional constraints on the Moho depths (e.g. see [*Hurtig et al.,* 1992; *Kostyuchenko et al.,* 1999] have significantly improved isostatic compensation models. Recent studies showed that the use of updated models can significantly change the notions of isostasy in various regions [*Artemjev and Kaban,* 1986, 1991; *Artemjev et al.,* 1994a, 1994b; *Kaban,* 1988], and this requires new calculation of isostatic gravity anomalies which can be regarded as a second main "geodynamic" reduction of the gravity field.

2. Principles of the Gravity Modeling

Main principles underlying the method used in this work can be formulated as follows. At the first stage, an initial density model of the crust and upper mantle whose parameters are determined from the available a priori data is constructed. This model consists of two layers representing the sedimentary cover and solid crust, whose parameters are basically different. More detailed division is impossible for such a vast territory because the basement and Moho interfaces are the only reference boundaries that are consistently identified by nearly all seismic methods.

The sedimentary layer is usually inhomogeneous in both vertical and lateral directions. Moreover, density variations within the sedimentary cover often produce much larger gravity effect than variations in the depth to basement. This effect is most distinct in the cases when the thickness of the sedimentary cover exceeds 7–8 km because the density of sediments near its base is close to the density of their host crystalline rocks. Major sedimentary basins have been studied in detail using various geophysical exploration methods and reference drilling data. Therefore, a general density

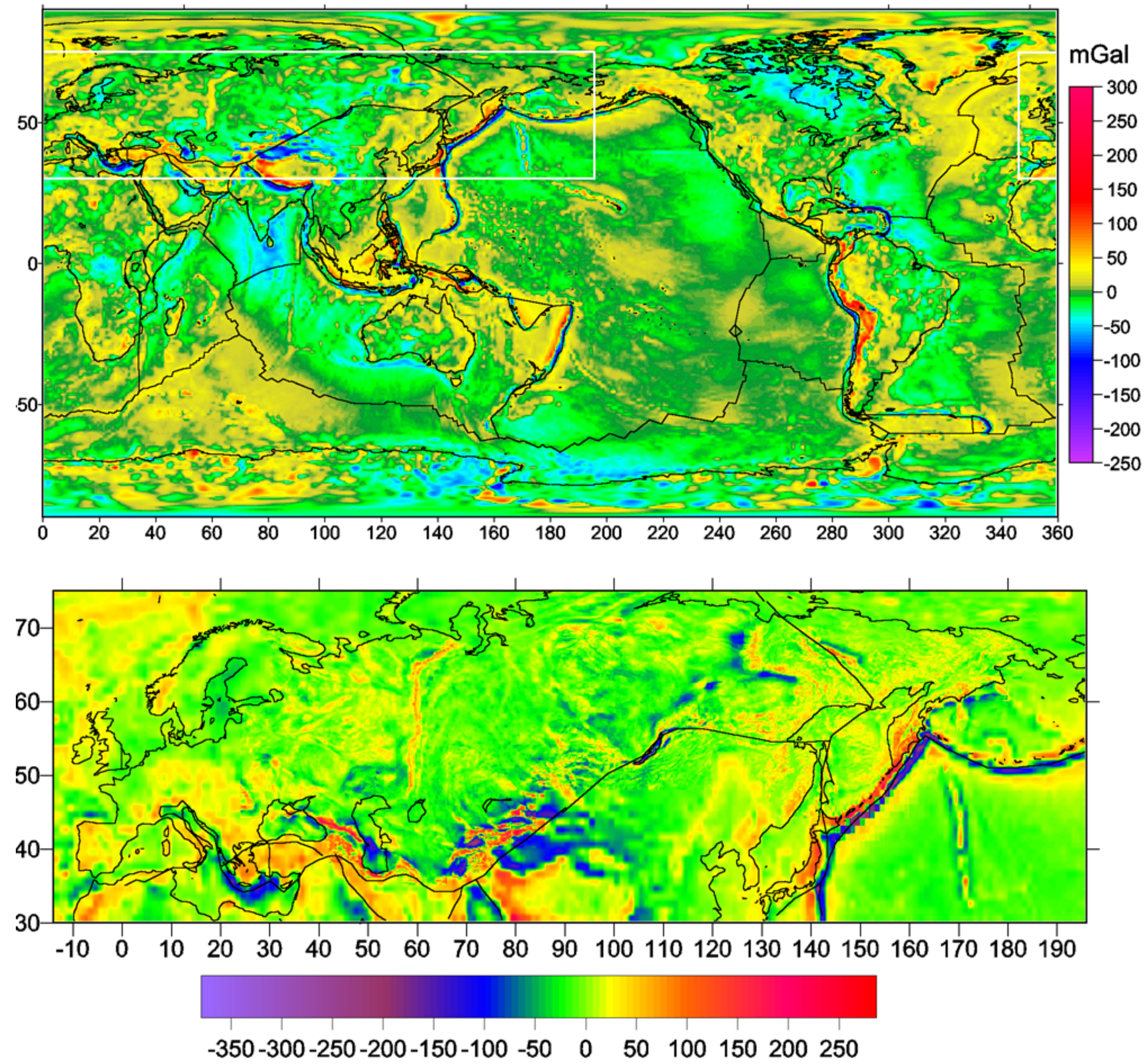

Figure 1. Free-air anomalies (in mGal): global view (top) and North Eurasia (bottom) [*Artemjev et al.,* 1994a, 1994b; *Lemoine et al.,* 1998].

model of the sedimentary cover can be constructed in principle without interpreting the gravity field.

Drilling data reveal a very intricate structure of the sedimentary sequence including numerous local boundaries [*Avchan and Ozerskaya,* 1985]. Attempts to incorporate these boundaries into a general model (at least for one sedimentary basin) have usually been unsuccessful. The only approach suitable for a regional study consists in the use of general patterns of the density variations with depth and in their correction accounting for the lithology of a specific basin. Thus, each sedimentary basin or, if necessary, its part is specified by a concrete depth dependence of the density of sediments. Possible (and often fairly large) deviations from the general dependence are of local nature and are outside the scope of this study. Such an approach was successfully applied by several authors and proved effective [*Artemyev et al.,* 1993; *Kaban and Mooney,* 2001; *Yegorova and Starostenko,* 1999]. In this work, the regional model of the sedimentary cover constructed in [*Artemjev et al.,* 1993, 1994a, 1994b; *Gordin and Kaban,* 1995] is used.

In principle, the effect of solid crust density inhomogeneities can also be estimated from data on average velocities of seismic waves. However, the reliability of this information is lower than the reliability of other datasets including constraints on the Moho boundary position. Only the data on various types of waves measured on long DSS pro-

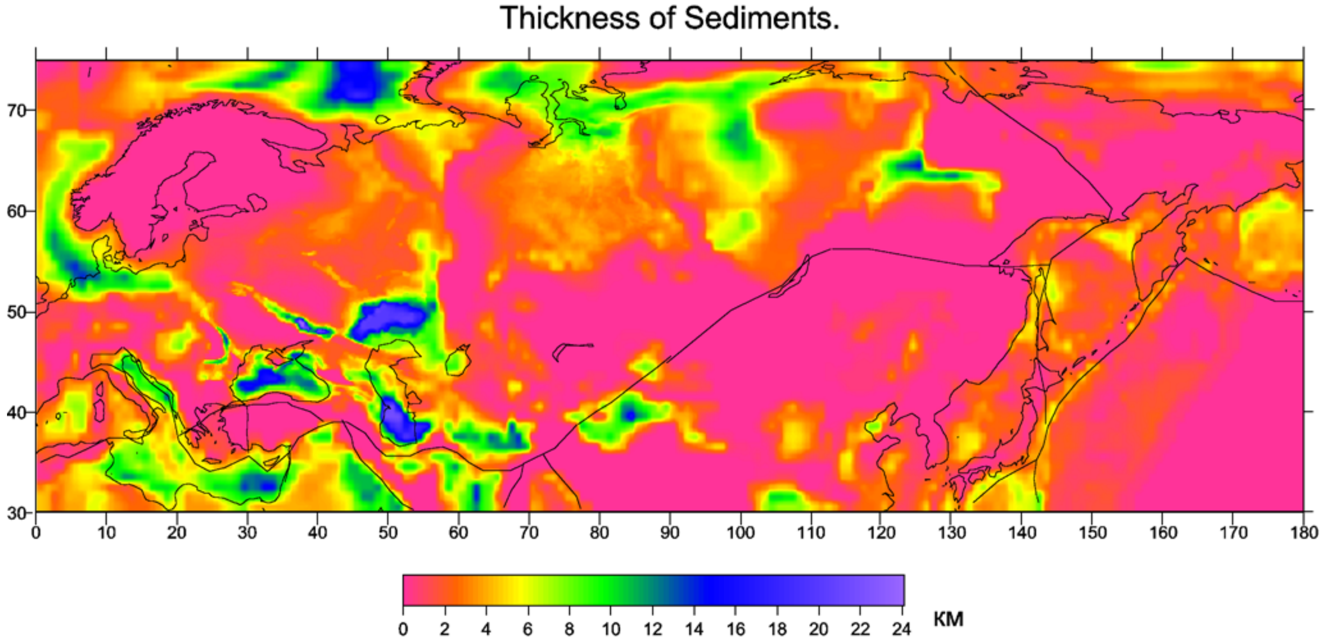

Figure 2. Depths to the basement (in km).

files (e.g., profiles measured by staff members of the GEON Center [*Egorkin,* 1991; *Kostyuchenko et al.,* 1999]) yielded a determination uncertainty of the average velocity significantly smaller than its variations in the solid crust. Importantly, this uncertainty can be systematic and dependent on the interpretation method in use. Moreover, the velocity into density conversion introduces an additional uncertainty [*Christensen and Mooney,* 1995; *Krasovskii,* 1989]. In view of the above arguments, two models of the crust were used. The solid crust density in the first model was set constant. Accordingly, the residual anomalies obtained upon the removal of the crust effect from the observed gravity field account for density inhomogeneities in both the upper mantle and solid crust. The second model accounts for the density inhomogeneities of the solid crust derived from seismic velocities. Comparison of these results enhances the reliability of final conclusions.

The gravity field of the initial crust model is calculated relative to a horizontally homogeneous reference model. If the lower boundary of the model is also horizontal, the resulting field, will be independent, accurate to a constant, of the choice of the reference model. In order to exclude from the consideration the lower boundary until which the calculations are performed, the reference model should meet the following single condition: the density of its mantle should be equal to the average mantle density adopted in the initial calculations. In this study, a two-layer reference model with densities of 2.7 g/cm^3 in the upper crust, 2.9 g/cm^3 in the lower crust, and 3.35 g/cm^3 in the mantle is used. The depth to the lower boundary is 34.3 km, coinciding with the average Moho depth within the region studied. The depth to the crustal density discontinuity (2.7/2.9 g/cm^3) is 14 km, giving an average crust density of 2.84 g/cm^3, which is consistent with worldwide data [*Mooney et al.,* 1998].

At the second stage, additional density inhomogeneities are introduced in the upper mantle under the condition of a vanishing sum of all anomalous masses in each lithosphere column down to a specified level, including both the a priori known (topography, sedimentary cover and solid crust down to Moho) and additional mantle compensating masses. The field produced by additional density inhomogeneities in the upper mantle is subtracted from mantle gravity anomalies; the resulting isostatic gravity anomalies may be regarded as the second major characteristic of the geodynamic regime of a tectonic structure.

3. Initial Data and the Reference Density Model of the Crust

Figure 1 presents the initial gravity field (free-air anomalies) in the region under study together with the global scheme. Since the resolution of the initial data sets varies significantly within this territory, the inferred results are also nonuniform. All transformations of gravity fields in a (14°W–180°E, 30°–75°N) area were performed with a 1°×1° resolution. The initial gravity field with such a resolution was taken from the EGM96 model [*Lemoine et al.,* 1998]. For a significant part of Eurasia including the former USSR territory, the available gravity data are more reliable and can be represented on a $10' \times 15'$ grid, which is of major importance for isostatic anomalies because much information is lost due to averaging. The initial field is represented by free-air anomalies with the terrain correction applied within an area of a 200-km radius (the so-called Fay anomalies).

Figure 2 presents a map showing depths to the basement. It is based on the map of *Artemjev et al.* [1994a], which was complemented using results of more detailed studies in the area adjacent to the Alpine foldbelt and central and southern parts of the East European platform [*Gordin and Kaban,* 1995; *Kaban et al.,* 1998] and in the West Siberian basin [*Artemjev et al.,* 1994b]. New data on the China territory were afforded by Chinese researchers within the framework of the joint project [*Feng et al.,* 1996]. The final map indicates that the thickness of sediments is greatest in the southern Caspian, Black and Barents seas, where it reaches 22–24 km. Characteristic relationships of density versus depth were determined for each sedimentary basin [*Artemjev et al.,* 1993, 1994a, 1994b; *Gordin and Kaban,* 1995]; the most typical of them are shown in Figure 3. The total gravity effect of the sedimentary cover relative to the laterally homogeneous reference model is shown in Figure 4. The major contribution is due to the upper sedimentary layer, where the effect was calculated relative to a density of 2.7 g/cm^3, and only in the deepest basins (South Caspian, Black Sea and Pre-Caspian) the effect of the deep roots is significant. The anomalous gravity field of sediments in these basins reaches –145 mGal. On the other hand, nearly the same effect in the West Siberian sedimentary basin is due to the upper low-density part of the sedimentary cover. The determination uncertainty of this field does not exceed 15% for relatively extended (more than a few hundred kilometers) structures. Of course some local sedimentary basins are not accounted for by this model, but their effect is easily recognized in the resulting isostatic anomalies.

Another important parameter estimated from the anomalous density of the sedimentary cover is the so-called adjusted topography. When calculating this parameter, water and sediments are numerically "compacted" to a normal density of the upper crust of 2.67 g/cm^3. The adjusted topography is an important parameter involved in many reconstructions (e.g. the calculation of isostatic anomalies). It is much more appropriate to use the adjusted, rather than observed, topography because it represents a homogeneous surface load. The map showing the adjusted topography for the entire territory of North Eurasia is presented in Figure 5.

Based on a synthesis of various seismic (mainly DSS) data, a map showing depths to Moho is constructed for the entire region under study (Figure 6). For the main part of Russia (except its northeastern part) the maps prepared at the GEON Center were used [*Egorkin,* 1991, 1998; *Kostyuchenko et al.,* 1999, 2000]. The data reported by *Hurtig et al.* [1992] for Western Europe, by *Kaban et al.* [1998] for the Caucasus – Kopet-Dag region and adjacent areas, by Levi (personal communication) for the Baikal region, and in [*Feng et al.,* 1996; *Lithospheric Dynamics...,* 1989] for China and Mongolia were incorporated.

Significant information can be recovered from the analysis of the relationship between variations in the surface load (adjusted topography) and Moho depth. This relationship served as a basis for using the Airy model in early isostatic studies [e.g., *Artemyev,* 1975]. However, in the early 1980s it became clear that the parameters characterizing the relationship between the topography and Moho are generally not the same for different types of structures and their variations are related to density properties of the lithosphere (e.g. see [*Artemyev and Golland,* 1983]). The data presented here

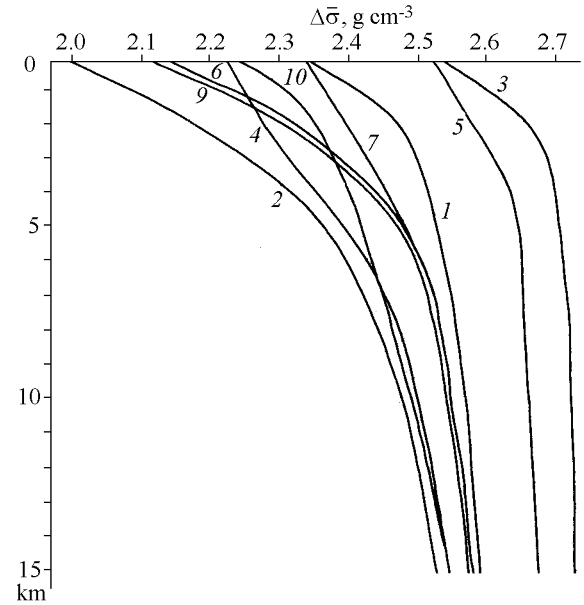

Figure 3. Generalized depth dependences of density of sediments in major basins.

on the adjusted topography and crustal thickness variations provide a new basis for the analysis of this problem.

Figure 7 presents the plot of the adjusted topography (t) versus crust-mantle boundary depth (M) for the continental North Eurasia. The correlation coefficient of these parameters amounts to 0.77 and the linear regression is described by the equation M = 5.9t + 37.8 (km). Considering that large lithospheric blocks for which this relation was obtained should be isostatically adjusted, the average density difference between the solid crust and upper mantle can be determined. This difference should amount to 0.45 g/cm^3, i.e. is equal to the density difference between the solid crust and subcrustal layer in the reference model. However, the points in Figure 7 show a large scatter indicating that this relation is violated for some structures.

Figure 8 presents a map showing the distribution of the "normal" thickness of the crust (i.e. thickness of a crust with zero adjusted topography) obtained by calculating the regression of the crustal thickness and residual topography in a moving window of an average radius of 7°. As discussed above, the "normal" crustal thickness is directly related to the average density of mantle. Its higher values correspond to higher densities of the lithosphere, which like an anchor prevents the crust from floating up and vice versa. As is shown below, the distribution of the "normal" crustal thickness is fully consistent with the distribution of the regional components of the residual mantle field.

The map showing the average P wave velocities in the solid crust of North Eurasia is presented in Figure 9. The territory of Russia is mostly mapped using the GEON Center data [*Egorkin,* 1991, 1998; *Kostyuchenko et al.,* 1999, 2000] complemented with the results of generalization made by *Volvovskii and Volvovskii* [1975]. The map of the Western Europe territory was constructed from data by *Gize and*

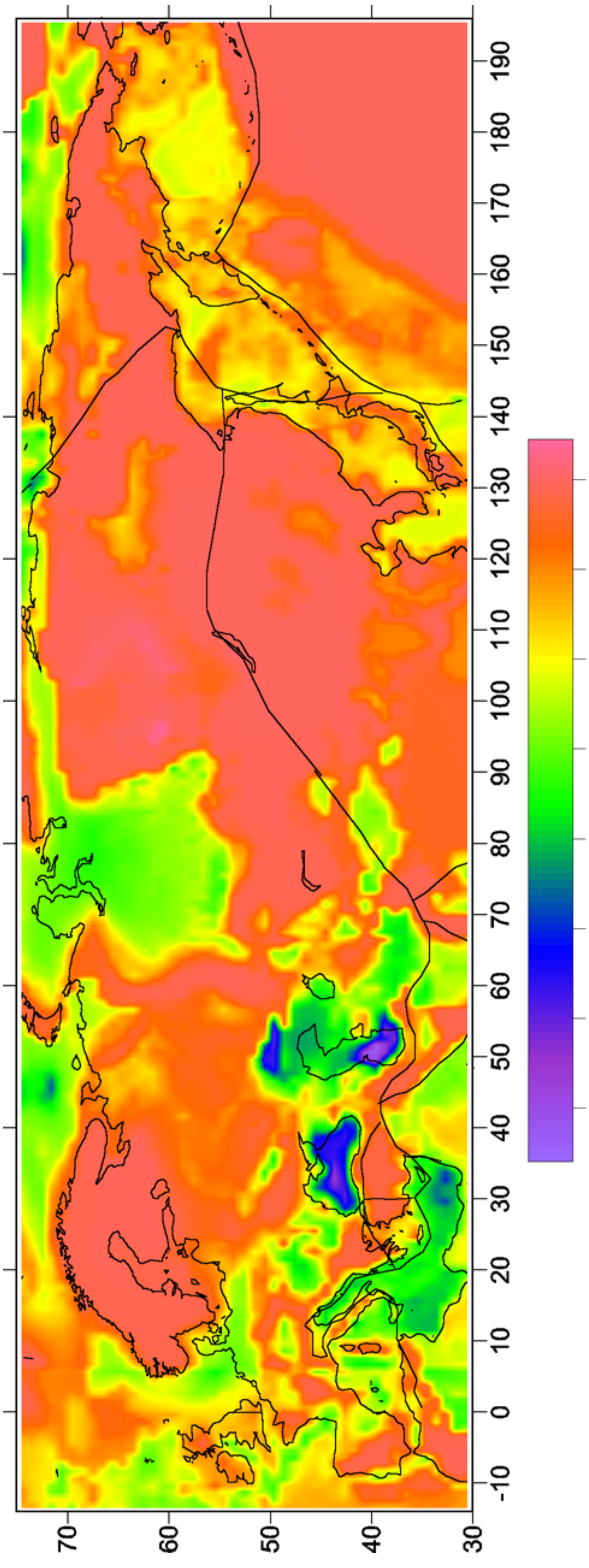

Figure 4. The total gravity effect (in mGal) of the sedimentary cover relative to the laterally homogeneous reference model.

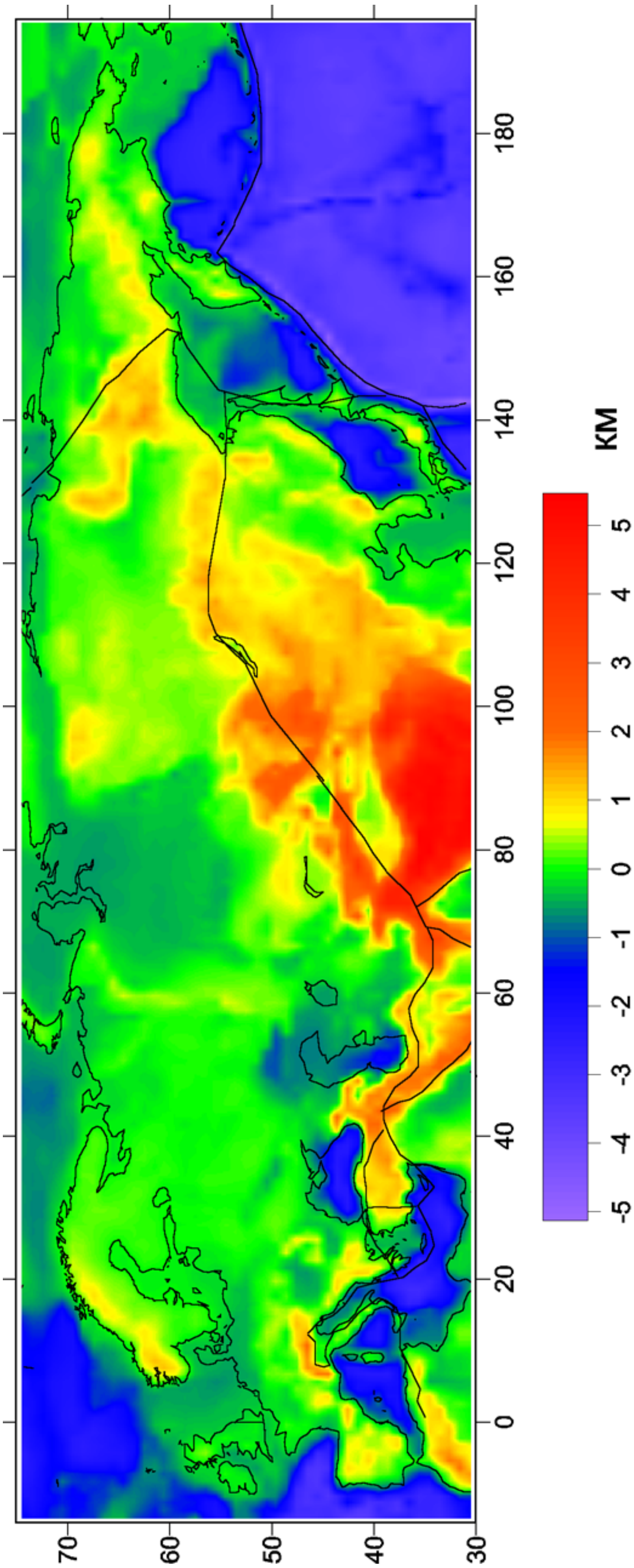

Figure 5. Map showing the adjusted topography (in km). When calculating this parameter, water and sediments were numerically "compressed" to a normal surface density of 2.67 g/cm^3.

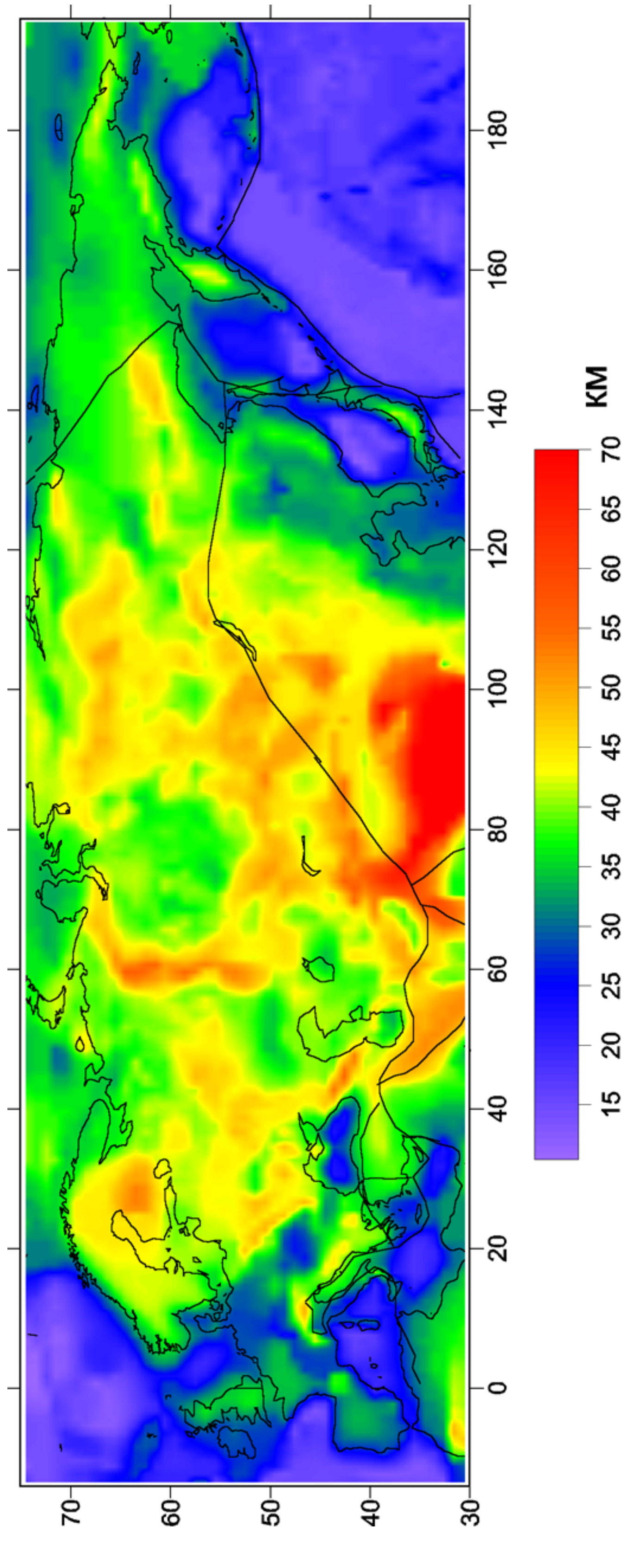

Figure 6. Moho depths relative the ocean level (in km).

=

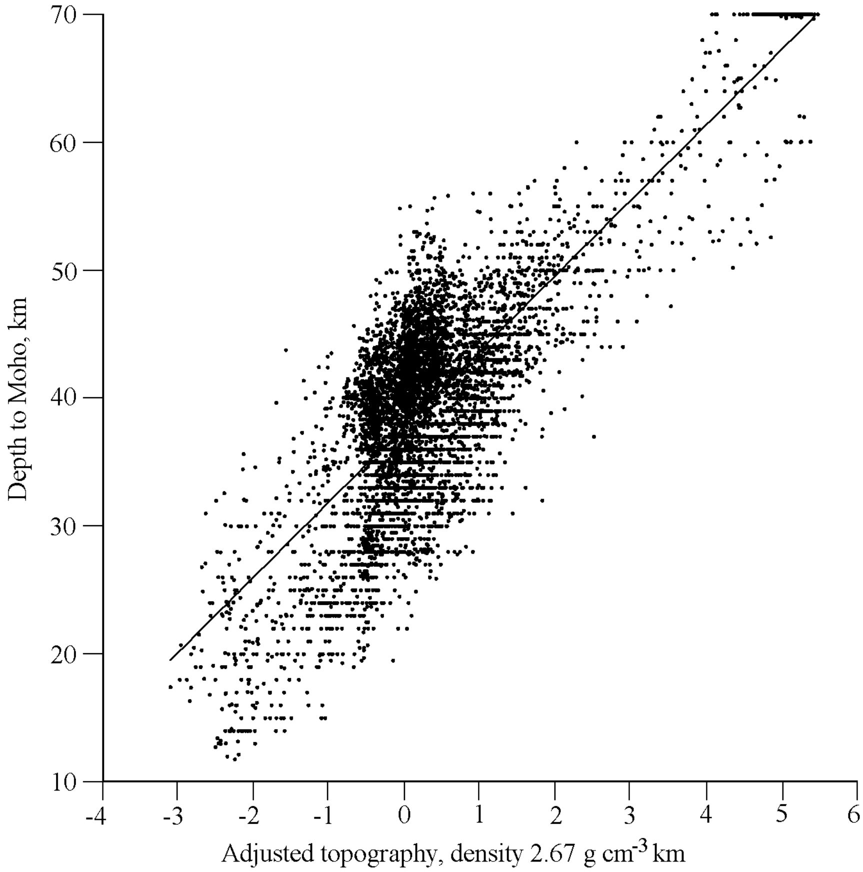

Figure 7. The relationship between the adjusted topography and the depth to Moho in continental North Eurasia.

Pavlenkova [1988]. The velocities in the remaining part of North Eurasia were taken from the global $5° \times 5°$ model of *Mooney et al.* [1998]. Average velocity variations in the solid crust are fairly large and range from 6.3 to 7 km/s, which may indicate significant density variations.

The problem of conversion of seismic velocities to densities does not have a unique solution [*Christensen and Mooney,* 1995; *Krasovskii,* 1989], although the relation between these parameters in solid crust rocks is more stable than in the sedimentary cover and upper mantle. In the present study, the velocity to density conversion relations derived by *Christensen and Mooney* [1995], allowing for possible differences in the rock composition (e.g. in oceanic and continental regions), are utilized. According to these authors, the possible uncertainty in the determination of density from P wave velocity on a regional scale (i.e. for relatively large structures) amounts to 0.05 g/cm^3 for a separate layer and 0.03 g/cm^3 for the solid crust as a whole. These values were used for estimating the reliability of results.

Figures 10 and 11 show the gravity effect of the solid crust including Moho variations. In the first case the solid crust density is set constant and equal to 2.84 g/cm^3. The map in Figure 11 shows the model field allowing for density variations in the solid crust. The "net" contribution of density variations ranges from -125 to $+160$ mGal, and its variations do not necessarily correlate with density variations, which is due to differences in the position of solid crust boundaries relative to the reference model boundaries. A relatively small density can produce a significant positive effect if a considerable portion of the crust overlies the upper part of the reference model having a density of 2.7 g/cm^3. Such a situation is typical of oceanic regions. Alternative cases are regions of the solid crust subsidence (for example, in the cis-Caspian basin) where the effect of higher density of the solid crust is compensated for by a high density of the reference model at these depths.

4. Residual (Mantle) Anomalies of the Gravity Field

The residual gravity anomalies shown in Figure 12 were obtained after the following effects had been removed from Bouguer anomalies: the anomalous gravity field of the sedimentary cover, the anomalies due to the Moho depth variations, and regional fields associated with effects of the most

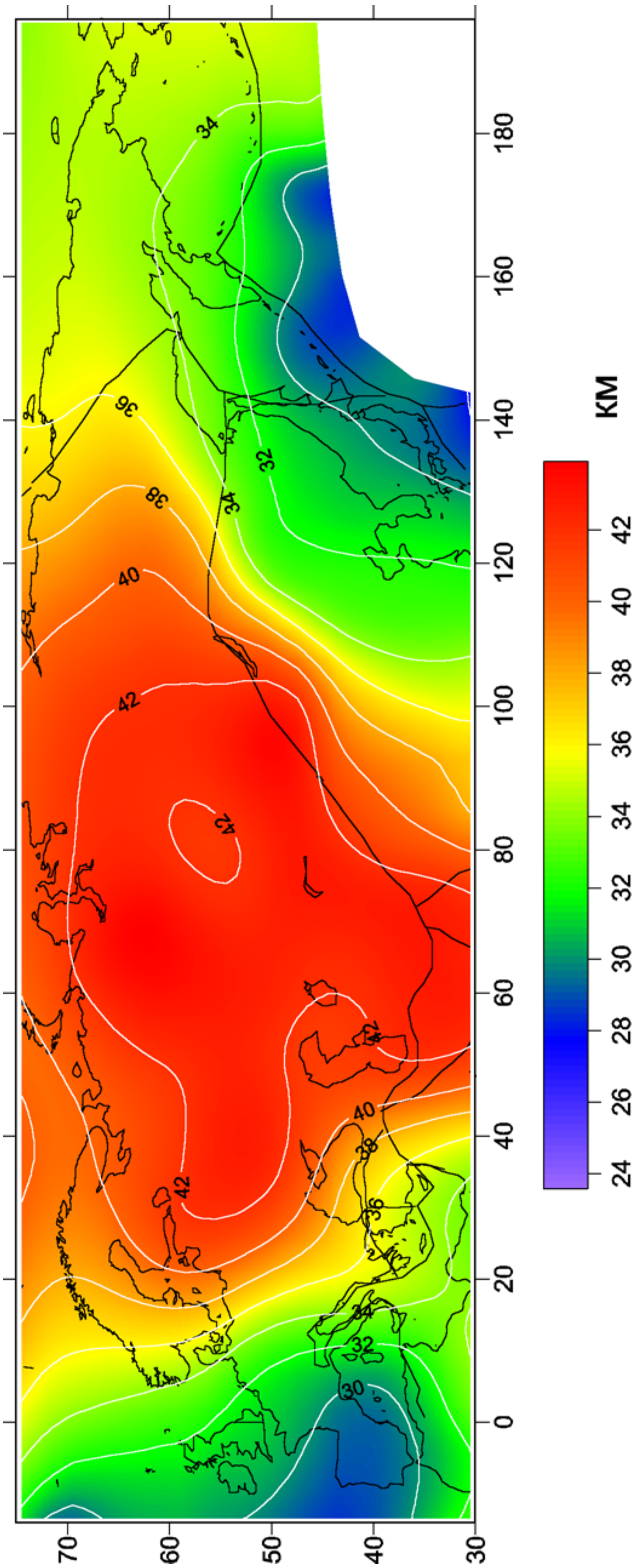

Figure 8. Map showing the distribution of the "normal" crustal thickness corresponding to a zero adjusted topography and obtained by calculating the regression of the Moho depth and adjusted topography in a moving window of a 7° radius.

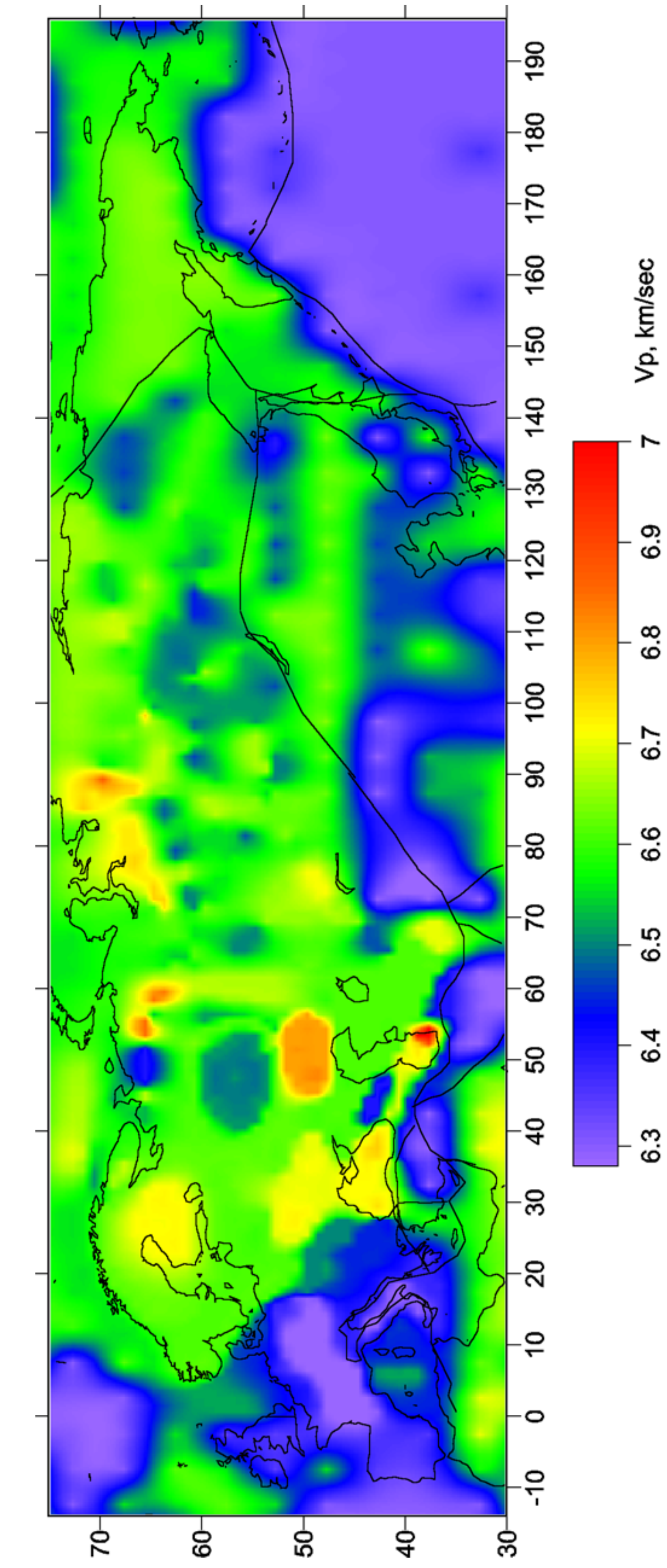

Figure 9. Map showing average P wave velocities in the solid crust of North Eurasia (in km/s).

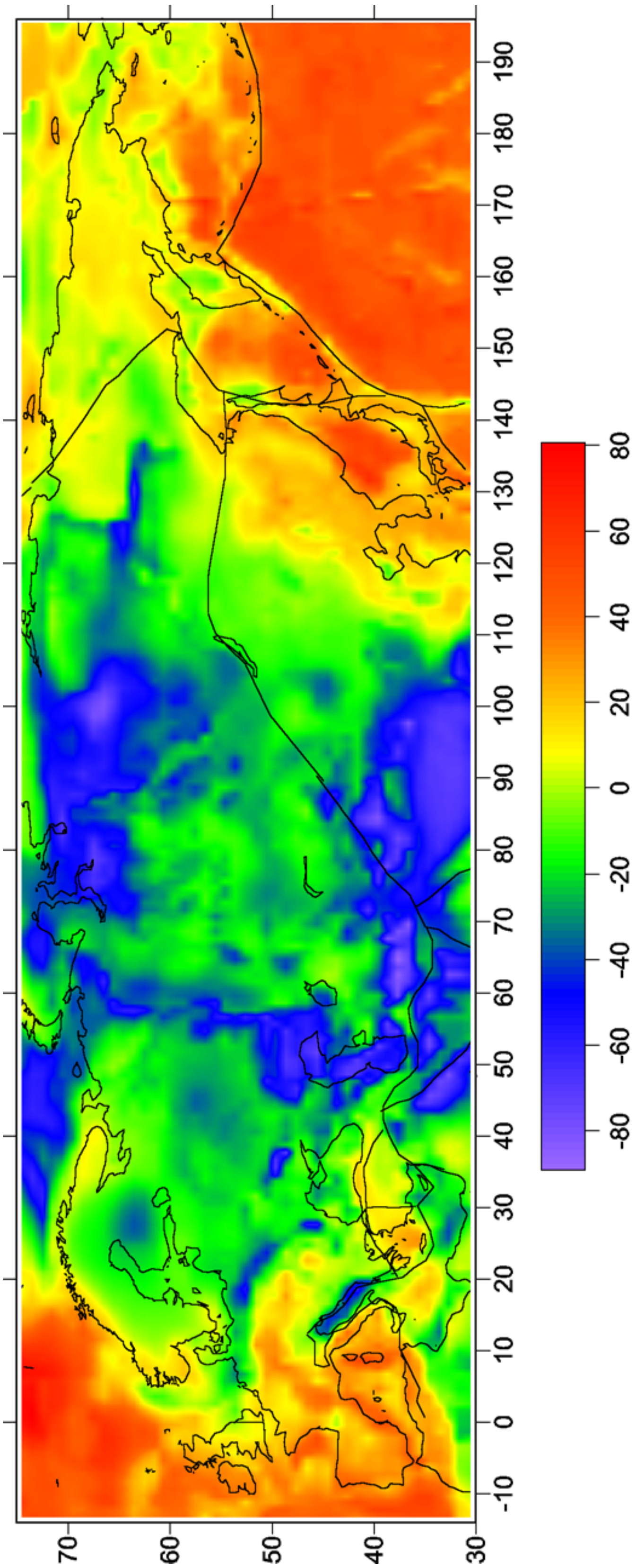

Figure 10. The gravity effect of the solid crust including Moho variations (in mGal). The solid crust density is constant and equal to 2.84 g/cm^3.

=

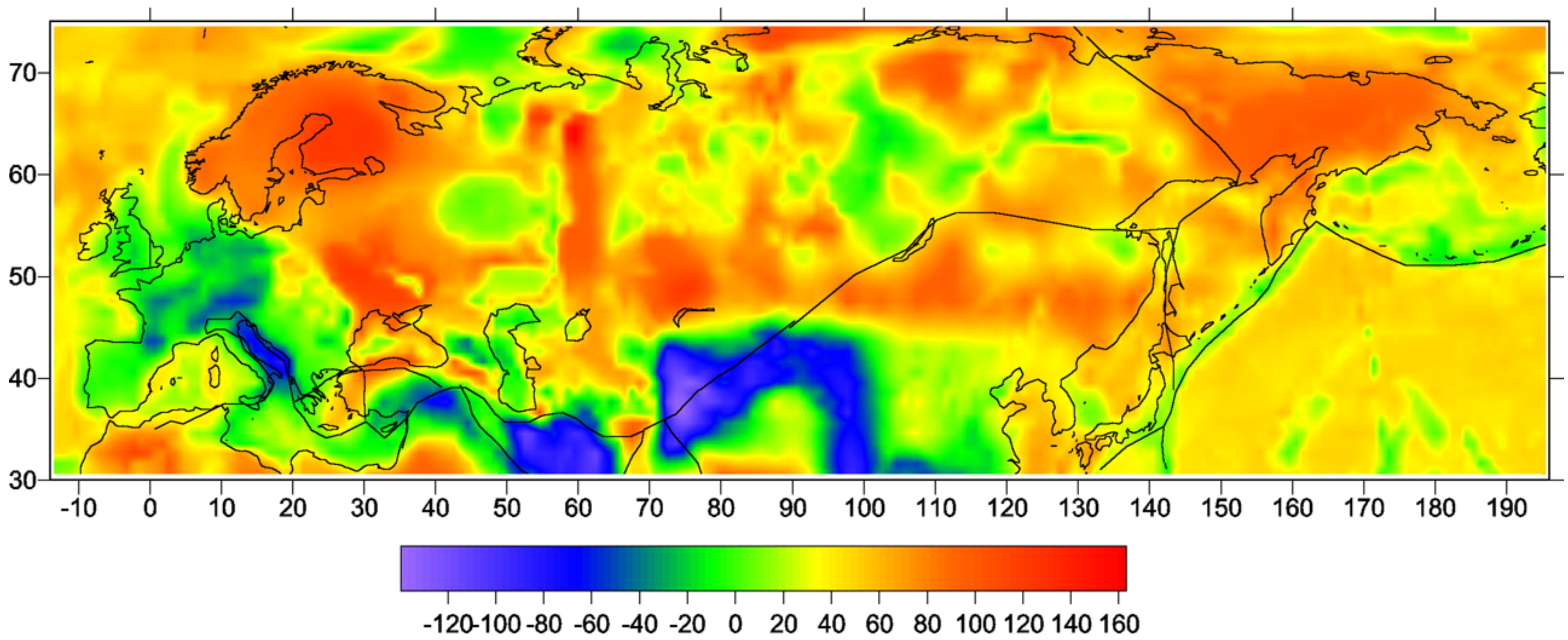

Figure 11. The gravity effect of the solid crust including Moho variations (in mGal). The solid crust density is calculated from the data on seismic velocities (Figure 9).

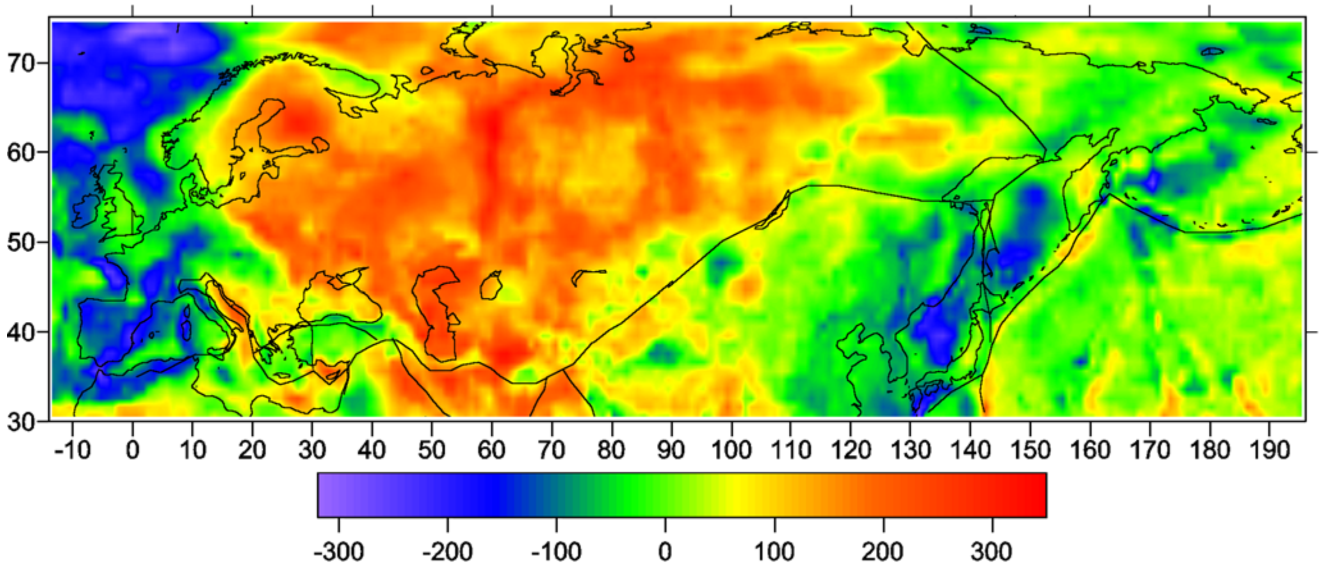

Figure 12. Residual gravity anomalies (in mGal) obtained after the following fields were subtracted from the Bouguer anomalies: the gravity field of the sedimentary cover, anomalies due to Moho depth variations, and regional fields produced by the most significant masses located outside the calculating area up to the antipodes (see the text). The solid crust density is constant and equal to 2.84 g/cm^3.

significant masses located outside the calculating area up to antipodes. The first two fields are computed at each point within a radius of 10 degrees.

Since the maximum depth to Moho does not exceed 70 km such a radius is sufficient to account for the crustal thickness and density variations with a sufficient accuracy. The regional fields represent the influence of topography and its compensation for the rest of the world. The influence of large structures (on a continent-ocean scale) can be significant even in the case of full isostatic compensation [*Artemjev et al.*, 1993, 1994a, 1994b]. Thus, if possible uncertainties in the initial data are not taken into account, these anomalies indicate the lateral heterogeneity of the solid crust and upper mantle. Figure 13 shows the same anomalies from which the gravity effect of solid crust density variations, determined in the previous section, was additionally removed. The comparison of Figures 12 and 13 shows that the crustal correction considerably decreases the amplitude of the re-

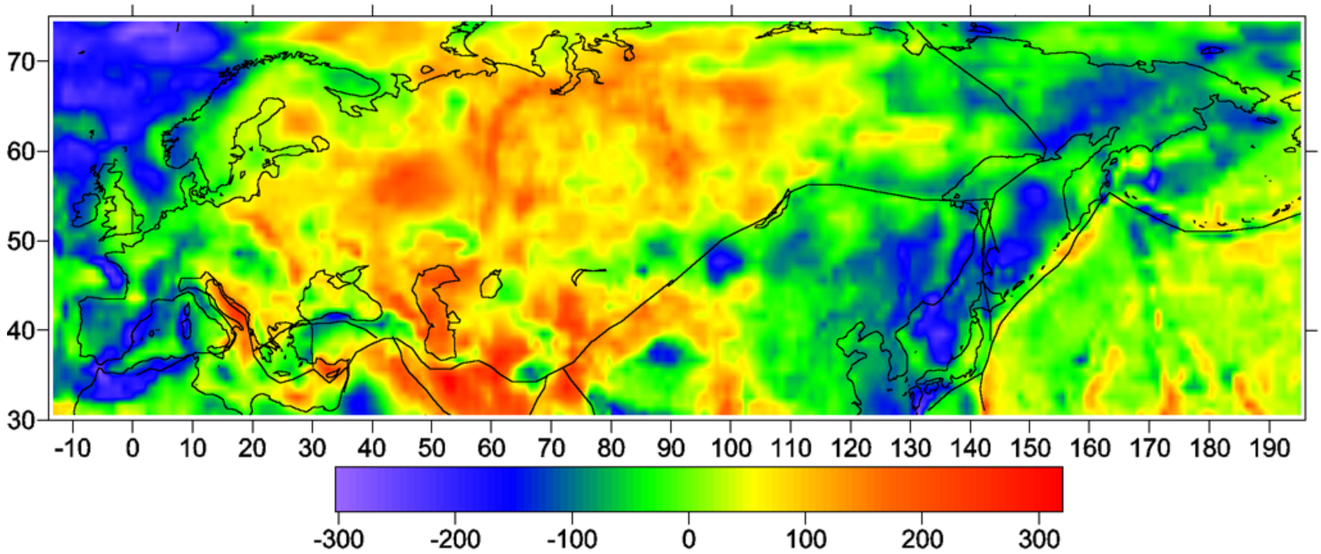

Figure 13. Residual mantle anomalies of the gravity field (in mGal). The gravity effect of the solid crust density variations, calculated from seismic velocities, was additionally eliminated from the field shown in Figure 12.

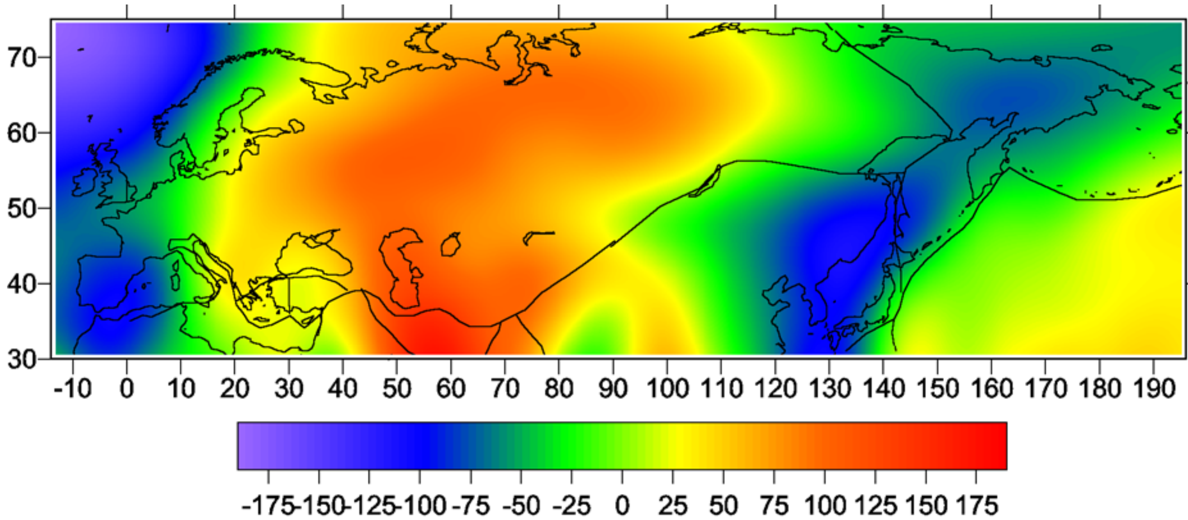

Figure 14. The regional component (wavelengths longer than 2400 km)) of the mantle gravity field shown in Figure 13. The values are given in mGal units.

gional component in the residual anomalies but does not change the general spatial pattern of the anomalies.

The mantle anomaly amplitudes in North Eurasia reach ±300 mGal, considerably exceeding their determination uncertainties that can attain 100 mGal in poorly studied areas and range from 25 to 50 mGal in other regions, depending on the crustal thickness. The most prominent feature of the resulting field is its distinct separation into the regional and local components shown in Figures 14 and 15. In a first approximation, the regional component does not correlate with the crustal structure: vast areas characterized by anomalies of predominantly the same sign include diverse structures. Intense positive anomalies with average amplitudes of 100–150 mGal are observed in northern and central Eurasia. This region is bounded in the west by the Tesseyre-Tornquist line, which is a “geophysical” (and “geological”) boundary between Western and Eastern Europe. This line can be continued to the southeast where it divides the Greater and Lesser Caucasus characterized by intense negative anomalies, although the anomalous field here may have quite a different origin as compared with Western Europe. To the east, the region of positive anomalies is bounded by a line trending from the southwest, where it divides the Afghan-Tajik depression overlying a very dense mantle and the Pamirs. This line extends further to the northeast along the northwestern boundary of the Sayany Mountains and Baikal rift zone and reaches the Eurasia boundary near the Tiksi area. It is still unclear to which megablock the Aldan Shield should be at-

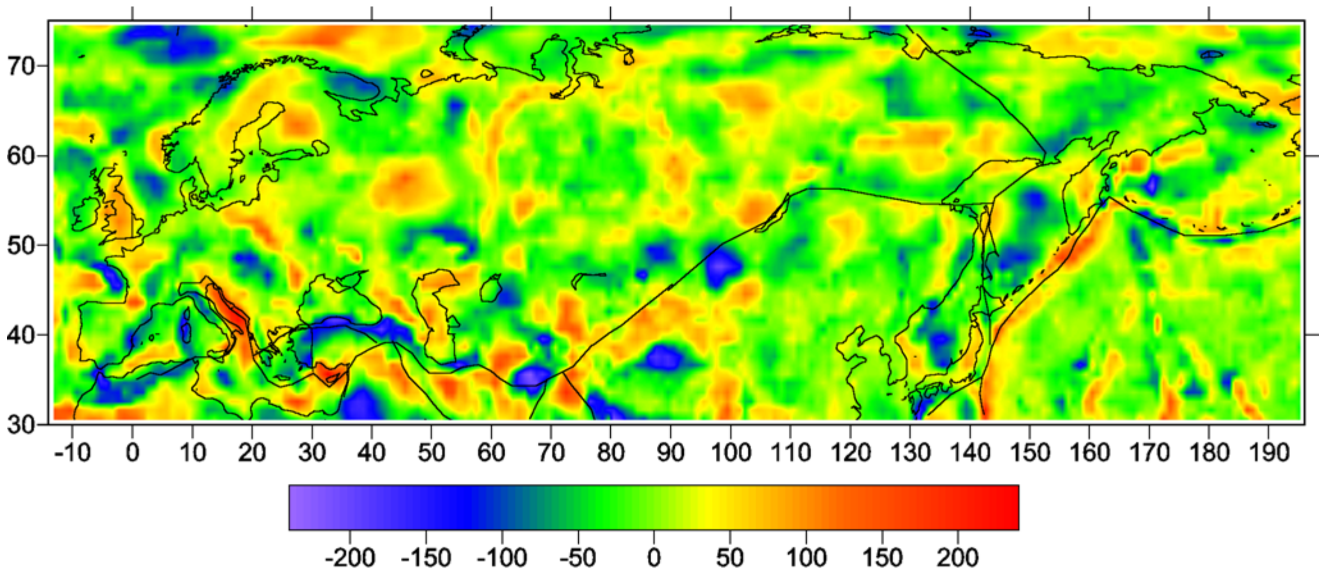

Figure 15. The short-wave (less than 2400 km) component of the mantle residual anomalies shown in Figure 13. The values are given in mGal units.

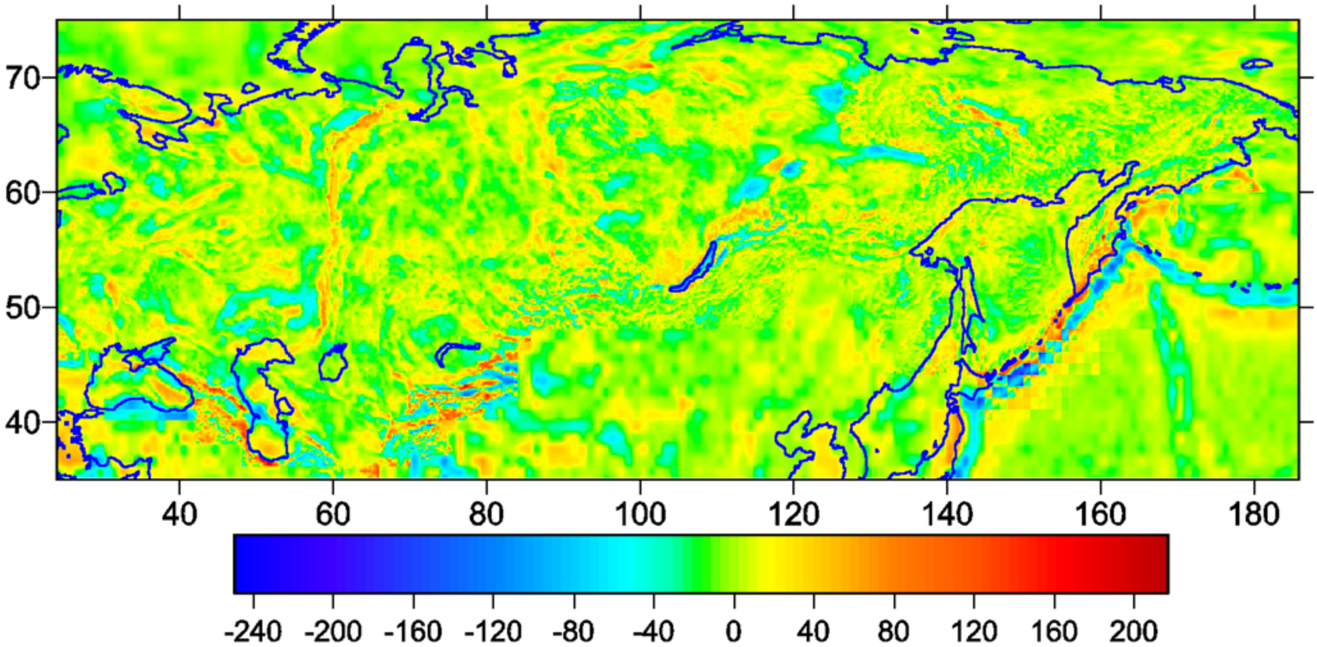

Figure 16. Local isostatic anomalies (wavelengths shorter than 2400 km). The values are given in mGal units.

tributed. The temperature field is likely to make the major contribution to the regional variations in the upper mantle density, which is supported by results of the surface wave interpretation [*Ekstrom and Dziewonski,* 1998; *Ritzwoller and Levshin,* 1998]. These authors discovered a high S wave velocity zone that extends to a depth of 250 km and exactly coincides with the above region of mostly positive residual mantle anomalies. Heat flow data also support this conclusion (a distinction between the thermal regimes of Western and Eastern Europe has been rather reliably established [*Cermak,* 1982; *Hurtig et al.,* 1992].

Unlike the regional field, the "local" residual anomalies with wavelengths of less than 2000–2500 km clearly correlate with tectonic structures (Figure 15). Local variations of mantle anomalies in platform regions are much smaller than in tectonically active regions. Positive anomalies are most pronounced east of the Tesseyre-Tornquist line. For example, shields of the East European platform are characterized

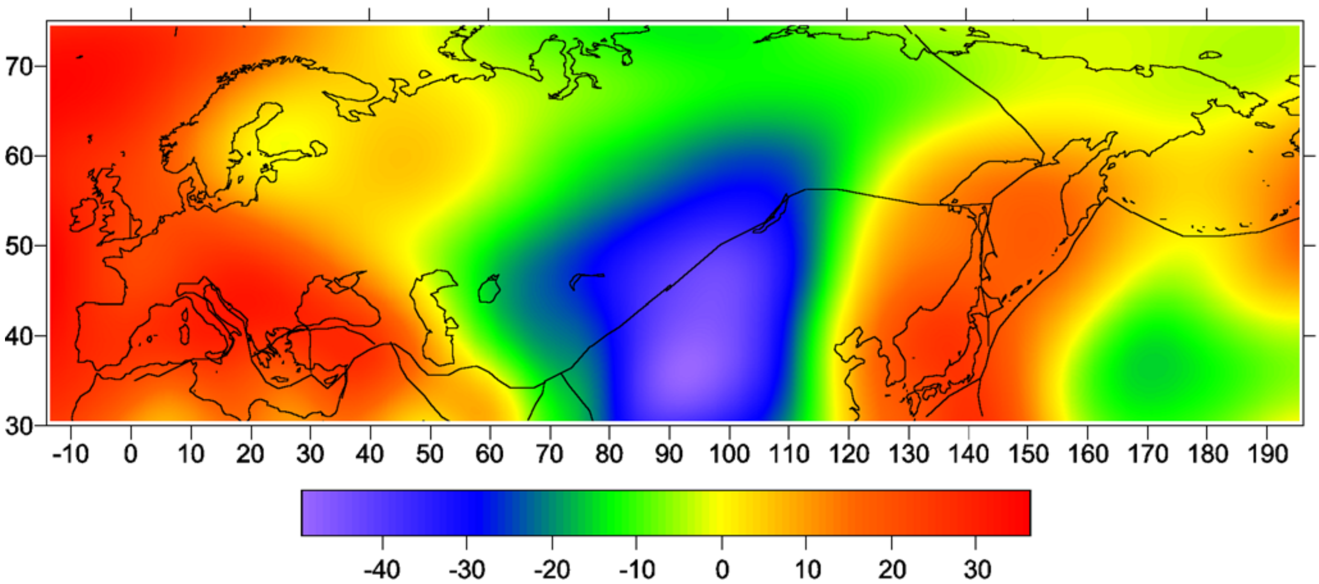

Figure 17. The regional component (wavelengths of more than 2400 km) of the isostatic anomalies. The values are given in mGal units.

by intense positive residual mantle anomalies with amplitudes of up to +100 mGal. A similar anomaly is observed in the eastern Urals (Magnitogorsk zone). Mantle anomaly values above the Tunguska syneclise reach +100 mGal, which is consistent with the upper mantle P wave velocities that are also very high in this region [*Deep Structure...,* 1991; *Egorkin,* 1998]. A chain of negative mantle anomalies is clearly traced west of the Tesseyre-Tornquist line (Pannonian basin-Rhine graben-Massif Central).

At first glance, the inferred results do not confirm the hypothesis proposed by several authors, according to which the density of the upper mantle is significantly smaller under the Black and southern Caspian seas (e.g. see [*Chekunov,* 1979]). However, very deep basement subsidences and Moho uplifts within these structures compensate for each other so that the mantle anomalies are close to zero over the Black Sea and have a noticeable maximum over the Caspian Sea.

The intense negative mantle anomalies observed along the eastern boundary of North Eurasia are associated with backar marginal seas. The deepest parts of these seas are also characterized by the most pronounced anomalies. The thermal origin of these negative anomalies is evident.

Two well-resolved zones of negative residual mantle anomalies are recognized in Central Asia. One of them is located southwest of Lake Baikal, approximately in the Khamar-Daban area. Unfortunately, since this region is poorly studied by seismic methods, this anomaly cannot be localized more accurately. However, there is evidence indicating that this region and a somewhat less distinct region of negative anomalies near the northeastern part of the Baikal rift zone are related to mantle plumes [*Grachev,* 1998]. Another zone of intense negative mantle anomalies is located in the Karakorum and primarily Kun Lun Mountains areas approximately between the Tarim basin and Tibet. Additional evidences required to elucidate the origin of these anomalies are unfortunately unavailable.

5. Isostatic Gravity Anomalies

Isostatic gravity anomalies are obtained as the difference between the observed gravity field and the field produced by an isostatically balanced lithosphere. In this study, the classical rigorous definition of isostasy is used, according to which the sum of anomalous masses in each lithospheric column above a certain depth, called the isostatic adjustment level, is zero. In addition to topography, anomalous masses of the sedimentary cover and Moho variations, density variations in the solid crust and upper mantle are introduced to obtain an isostatically balanced lithospheric column.

The resulting isostatic gravity anomalies are shown in Figure 16. The regional long wavelength component shown in Figure 17 was removed from these anomalies. The parameters used for separating short- and long-wave components of the isostatic anomalous field were chosen by analyzing the total field spectrum shown in Figure 18. This spectrum has a well-expressed minimum at wavelengths of 2000–2700 km. Obviously, structures with horizontal sizes of 1000 km and more are isostatically balanced regardless of the compensation model which plays no role at such wavelengths: isostatic anomalies at such wavelengths should be close to zero in any case. Thus, the long-wave component of the isostatic anomalies (Figure 17) is due to deep density inhomogeneities and dynamic effects of mantle convection flows. In the initial gravity field, these effects are almost completely masked by the field produced by lithospheric inhomogeneities. The gravity field of these inhomogeneities has a wide spectrum and cannot therefore be completely reduced by means of low-pass filtering [*Artemjev et al.,* 1994a, 1994b]. Thus, the long-wave anomalies obtained in this work are much more suitable for studying deep mantle heterogeneities and mantle convection than the long-wave component of free-air anomalies.

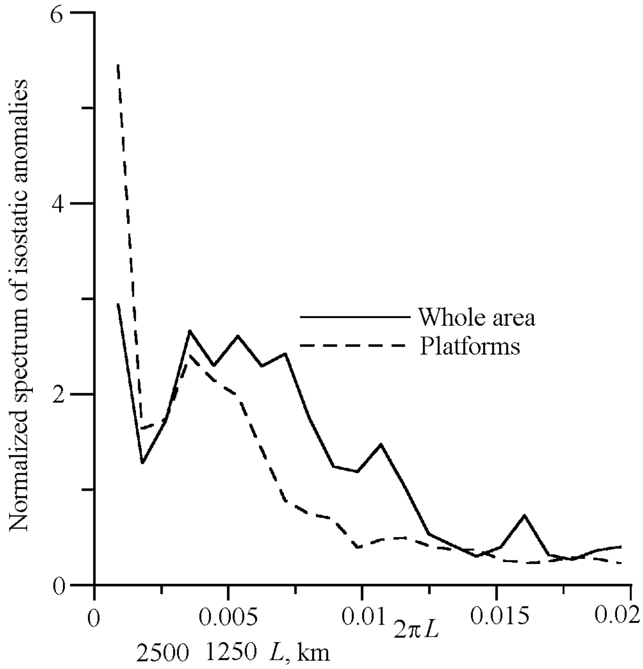

Figure 18. The spectrum of the isostatic anomalies of the gravity field.

Local isostatic anomalies (Figure 16) mainly reflect the effects of three factors:

1. Isostatic disturbances due to the possible elastic support of the surface load and to the effect of mantle flows.

2. Density inhomogeneities in the sedimentary cover and basement that are not accounted for in the model.

3. Differences between the actual and model schemes of isostatic adjustment.

In this study, the effects of the second and third factors are considerably reduced (at least for large structures) due to the inclusion of the sedimentary cover density inhomogeneities and determination of an effective isostatic compensation model. Thus, the isostatic anomalies derived in this work ensure much better resolution of geodynamic pattern as compared with the previous studies.

The intensity (variability) of the isostatic anomalies is directly related to the intensity of (present and past) tectonic activity in a specific region. The standard deviation of the

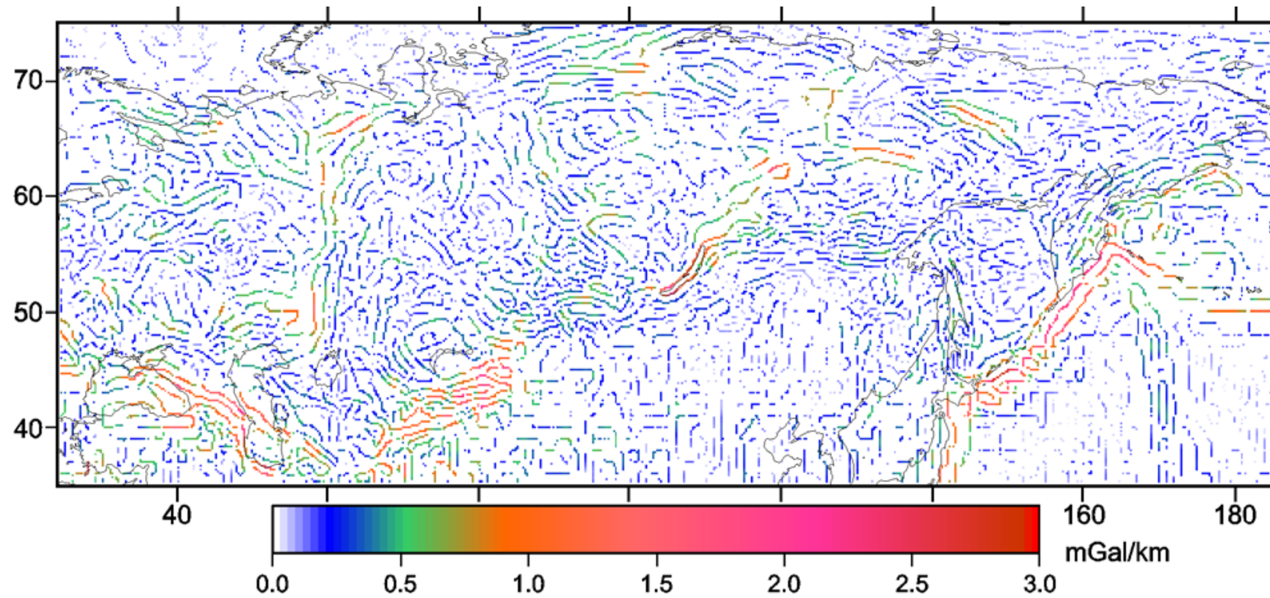

Figure 19. Horizontal gradient maximums (in mGal/km) of the isostatic anomalies, outlining the division of the lithosphere into blocks (see the text).

field shown in Figure 16 is 10–16 mGal in platform regions, 18–20 mGal in regions where mountains formed long ago (e.g. the Urals), 36–57 mGal in areas with a high level of the recent tectonic activity (Alpine-Mediterranean foldbelt and Pamir-Altai, Tien Shan and Baikal regions) and reaches 70 mGal in the island arc and deep trench areas. Note that the incorporation of the actual structure of the crust has substantially reduced (by a factor of up to 2) the amplitudes of isostatic anomalies as compared with the model calculated according to the simplest Airy scheme and using solely topographic data [*Artemyev,* 1975]. A more detailed analysis of the isostatic anomalous field will be presented in the next part of this paper.

Based on the inferred isostatic anomalies, maximum moduli of their lateral gradients are calculated (Figure 19). These gradients exhibit a fairly intricate pattern. A clearly recognizable superposition of gradient zones differing in intensity and width is evidence of a complex, hierarchically organized structure of the Eurasia crust. In order to delineate boundaries between blocks, the values of horizontal gradients of isostatic anomalies are determined, which are greater than their neighbours along at least two out of four possible directions. Nearly everywhere these values combine to form extended zones that should be regarded as block boundaries.

Gradient zones of the isostatic anomalies mostly delineate subvertical contacts of crustal rocks differing in density. Naturally, the majority of large faults should produce such contacts. In general, the lateral distribution of the zones supports this assumption. Furthermore, density contrasts across the faults in tectonically active regions should apparently be more expressed due to wider variety of rocks displaced by tectonic motions to different depths. Ancient deep faults in stable regions are buried under sediments and typically cut a basement surface strongly affected by denudation. Accordingly, the related gradient zones should be less intense. Thus, one may suppose that higher intensity fault zones are recognized in active regions, whereas stable regions include either ancient (dead) or passive fault zones. This conclusion is supported even by such example as the Urals Range: notwithstanding the widespread idea of very high gradients inherent in the field associated with contrasting density inhomogeneities in the Magnitogorsk zone, real gradients of isostatic anomalies there are significantly smaller than in tectonically active regions.

The above results lead to the conclusion that the gradient zones inferred in this work are authentic and reflect large fault zones (rather than the faults proper) which correspond to relatively extended deformation areas of the crust.

6. Conclusion

A density model of the North Eurasia crust is constructed and its gravity effect is calculated. The removal of this effect from the observed gravity field yielded residual mantle anomalies. They are reliably separated into two components reflecting the effects of the following factors.

1. The regional component does not correlate, in a first approximation, with the crustal structures and reflects large-scale structural features of the Eurasia lithosphere, supposedly related to its thermal regime. In particular, an intense positive anomaly is discovered in northern and central Eurasia, whereas negative anomalies are observed in Western Europe and Southeastern Asia. The regional component of the mantle gravity anomalies correlates well with the distribution of S wave velocities obtained by means of seismic tomography [*Ekstrom and Dziewonski,* 1998; *Ritzwoller and Levshin,* 1998].

2. As distinct from the regional component, the local component of the mantle anomalies with wavelengths shorter than 2000–2500 km clearly correlates with specific tectonic structures. The most pronounced positive anomalies with amplitudes exceeding 100 mGal characterize some structures of the East European platform (Baltic Shield and Voronezh Massif) and East Siberia (Tunguska syneclise). A chain of negative mantle anomalies is clearly traced west of the Tesseyre-Tornquist line (Hungarian basin-Rhine graben-Massif Central). The most prominent zone of negative mantle anomalies in Central Asia is located southwest of the Baikal rift zone, approximately in the Khamar-Daban area. These anomalies are likely to associated with intrusion of the anomalously light mantle. Intense negative mantle anomalies observed along the eastern boundary of Eurasia are related to backarc marginal seas.

A new map of the isostatic gravity anomalies is constructed throughout the territory studied. As distinct from previous studies, its calculation used real data on the crustal structure, including variations in the thickness and density of the sedimentary cover and solid crust. The use of these data instead of the traditional Airy scheme has led in many cases to a revision of notions concerning the isostatic state of crustal structures. In particular, the isostatic anomalies calculated for the South Caspian, Tien Shan and Urals regions are considerably reduced as compared with previous maps (e.g. see [*Artemyev,* 1975]). A joint analysis of the mantle and isostatic gravity anomalies intended to gain constraints on geodynamic settings of major tectonic structures in North Eurasia is a subject of the next stage of this study.

Acknowledgments. I am grateful to A. F. Grachev for fruitful discussions and help. This work was supported by Russian Foundation for Basic Research, project no. 01-05-64381.

References

Artemyev, M. E., *Isostasy in the Territory of the USSR,* Nauka, Moscow, 1975 (in Russian).

Artemyev, M. E., and V. E. Golland, Isostatic compensation of Tien Shan; choice of compensation model, *Phys. Solid Earth, 19,* 30–37, 1983.

Artemjev, M. E., and M. K. Kaban, The free mantle surface - new possibilities to reveal subcrustal inhomogeneities from the structure of the Earth crust, *J. Geodynam., 5,* 25–44, 1986.

Artemjev, M. E., and M. K. Kaban, Isostatic processes and intracontinental orogenesis, *J. Geodynam., 13,* 77–86, 1991.

Artemjev, M. E., and M. K. Kaban, Density inhomogeneities, isostasy and flexural rigidity of the lithosphere in the Transcaspian region, *Tectonophysics, 240,* 281–297, 1994.

Artemjev, M. E., G. V. Demjanov, M. K. Kaban, and V. A. Kucherinenko, Gravity field of the lithosphere density inhomogeneities of Northern Eurasia, *Phys. Solid Earth,* (5), 12–22, 1993.

Artemjev, M. E., M. K. Kaban, V. A. Kucherinenko, et al., Subcrustal density inhomogeneities of the Northern Eurasia as derived from the gravity data and isostatic models of the lithosphere, *Tectonophysics, 240,* 248–280, 1994a.

Artemjev, M. E., V. M. Gordin, M. K. Kaban, et al., *West Siberian Basin Basement Tectonic Segmentation. Final Report,* Woods Hole Oceanographic Institution, USA and Inst. of Physics of the Earth, Moscow, Russia, 1994b.

Avchan, G. M. and M. L. Ozerskaya, *Petrophysical Characteristic of the Sedimentary Cover in Oil and Gas Bearing Provinces of the USSR,* Nedra, Moscow, 1985 (in Russian).

Belousov, V. V, and N. I. Pavlenkova, Structure of the Europe crust from seismic data, in *Lithosphere of Central and Eastern Europe,* edited by A. V. Chekunov, Naukova Dumka, Kiev, 1993 (in Russian).

Bronguleev, V. V., Ed., *The 1:5,000,000 Map of the Pre-Riphean Basement Surface of the East European Platform,* Mingeo SSSR, 1986 (in Russian).

Cermak, V., A geothermal model of the lithosphere and a map of the thickness of the lithosphere on the territory of the USSR, *Phys. Solid Earth, 18,* 18–27, 1982.

Chekunov, A. V., Ed., *Gravity Model of the Crust and Upper Mantle,* Naukova Dumka, Kiev, 1979 (in Russian).

Christensen, N. I., and W. D. Mooney, Seismic velocity structure and composition of the continental crust: A global view, *J. Geophys. Res., 100B,* 9761–9788, 1995.

Deep Structure of the USSR, Nauka, Moscow, 1991 (in Russian).

Egorkin, A. V., Structure of the crust from seismic geotraverse measurements, in *Deep Structure of the USSR,* p. 118–134, Nauka, Moscow, 1991 (in Russian).

Egorkin, A. V., Velocity structure, composition and discrimination of crustal provinces in the former Soviet Union, *Tectonophysics, 298,* (4), 395–404, 1998.

Ekstrom, G., and A. M. Dziewonski, The unique anisotropy of the Pacific upper mantle, *Nature, 394,* 168–172, 1998.

Ermakov, V. B., G. V. Krasnopevtseva, V. N. Semov, and Yu. K. Shchukin, *Atlas of Maps Showing the Deep Structure of the Crust and Upper Mantle in the USSR,* VNIIGeofizika, Moscow, 1989 (in Russian).

Feng, R., V. M. Gordin, M. K. Kaban, and Y. Wang, Gravity field and the mantle inhomogeneities in Central Asia, *30th Intern. Geological Congr. Abstracts,* Beijing, vol. 1, p. 152, 1996.

Gize, P., and N. I. Pavlenkova, Structural maps of the Europe crust, *Fiz. Zemli,* (10), 3–14, 1988 (in Russian).

Gordin, V. M., and M. K. Kaban, *Isostatic residual and decompensated gravity anomalies and gravity data on the upper crust heterogeneities (central and southern parts of the East-European platform and the Caucasus). Final report,* Mobil Oil and Zonenshain Centre for Russian Geology and Tectonic, Univ. of Texas, Arlington, 1995.

Grachev, A. F., Gravity signatures of major neotectonic structural forms, in *Geomorphology and Geophysics,* edited by A. F. Grachev and L. Kulakov, p. 5–32, Nauka, Leningrad, 1972 (in Russian).

Grachev, A. F., The Khamar-Daban Ridge as a hotspot of the Baikal Rift from data of chemical geodynamics, *Phys. Solid Earth, 34,* 175–200, 1998.

Hurtig, E., V. Cermak, R. Haenel, and V. Zui, (eds.), *Geothermal atlas of Europe,* 1st ed., Hermann Haack Verlagsgesellschaft, 1992.

Kaban, M. K., *Study of the Lithosphere Isostasy,* Nauka, Moscow, 1988 (in Russian).

Kaban, M. K, M. E. Artemjev, A. I. Karaev, and A. P. Belov, The deep structure and geodynamics of the tectonic features in Turkmenistan and adjacent areas; gravity evidence, *Geotectonics, 32,* 323–332, 1998.

Kaban, M. K., and W. D. Mooney, Density structure of the lithosphere in the South-Western U.S. and its tectonic significance, *J. Geophys. Res., 106,* 721–740, 2001.

Kostyuchenko, S. L., A. V. Egorkin, and L. N. Solodilov, Structure and genetic mechanisms of the Precambrian rifts of the East-European Platform in Russia by integrated study of seismic, gravity, and magnetic data, *Tectonophysics, 313,* 9–28, 1999.

Kostyuchenko, S. L., L. N. Solodilov, and A. V. Egorkin, Characteristics of the structure and physical fields of the crust and upper mantle, in *Neotectonics Geodynamics and Seismicity of Northern Eurasia,* edited by A. F. Grachev, p. 291–308, Moscow, 2000.

Krasovskii, S. S., *Gravity Modeling of the Crust with Implications for Isostasy,* Naukova Dumka, Kiev, 1989 (in Russian).

Kusznir, N. J., The distribution of stress with depth in the lithosphere: thermo- rheological and geodynamic constraints, *Phil. Trans. R. Soc. Lond., 337,* 95–110, 1991.

Lemoine, F. G., N. K. Pavlis, S. C. Kenyon, et al., New high-resolution model developed for Earth's gravitational field, *EOS Trans. Am. Geophys. Un., 79,* 113–118, 1998.

Lithospheric Dynamics Atlas of China, China Cartographic Publishing House, Beijing, 1989.

Mooney, W. D., G. Laske, and T. G. Masters, CRUST 5.1: A global crustal model at $5° \times 5°$, *J. Geophys. Res., 103B,* 727–747, 1998.

Nevolin, N. V., and Kovylin, Eds., *Geological and Geophysical Modeling of Oil and Gas Bearing Provinces,* Nedra, Moscow, 1993 (in Russian).

Ritzwoller, M. H., and A. L. Levshin, Eurasian surface wave tomography: Group velocities, *J. Geophys. Res., 103,* 4839–4878, 1998.

Volvovskii, I. S., and B. S. Volvovskii, *Crustal Sections in the USSR from Deep Seismic Soundings,* Sovetskoe Radio, Moscow, 1975 (in Russian).

Yegorkin, A. V., and A. V. Mikhaltsev, The results of seismic investigations along geotraverses, in *Superdeep Continental Drilling and Deep Geophysical Sounding,* edited by K. Fuchs, Ye. A. Kozlovsky, A. I. Krivtzov, and M. D. Zoback, p. 11–119, Springer-Verlag, Heidelberg, 1990.

Yegorova, T. P., and V. I. Starostenko, Large-scale three-dimensional gravity analysis of the lithosphere below the transition zone from Western Europe to the East European Platform, *Tectonophysics, 314,* 83–100, 1999.

(Received August 10, 2001)